Land Degradation Classification of Coal Mine Area in the Loess Plateau Using Remote Sensing

Haochen Yu[1,2,3], Shouguo Mu[1,2,3,a,*], Jing Hou[1,2,3], Zhengfu Bian[1,2,3], Jiu Huang[1,2,3], Shaogang Lei[1,2,3] and Hao Chen[4]

[1]School of Environment Science and Spatial Informatics, China University of Mining and Technology, Xuzhou, China
[2]Collaborative Innovation Center for Resource Utilization and Ecological Restoration of Old Industrial Base in Jiangsu, Xuzhou, China
[3]Engineering Research Center of Mine Ecological Construction, Ministry of Education, China University of Mining and Technology, Xuzhou, China
[4]Land Resources Bureau of Xinyi, Xuzhou, China
a. mushouguo@163.com
[*]Corresponding author: Shouguo Mu

Keywords: Land degradation, remote Sensing, classification model.

Abstract: The ecological environment of the Loess Plateau is fragile. Land degradation could be easily caused due to the high-intensity mining surface disturbance, resulting in ecological damage and environmental pollution. Xunyao mining area was taken as a study area. Three main characteristics of vegetation coverage, desertification, and soil erosion were selected for Principal Component Analysis (PCA) based on the NDVI value. According to the weighted result, the land degradation classification model was constructed, and the land degradation results were obtained and graded. The main conclusions include (1)Soil erosion, vegetation coverage and desertification account for the external characterization weight of 0.6966:0.1828:0.1206. While soil erosion is the main characterization. (2)In 2013~2017, vegetation coverage, desertification, soil erosion, and land degradation all showed good in the southeast but poor in the northwest. (3) The low vegetation coverage and the desertification are mainly concentrated in the mining area; soil erosion not only affects the scope of the coal mine but also the range of the unmined area. Land degradation mainly caused by the surface disturbance for coal mining and the special fragile ecological environment in the Loess Plateau. The study could provide theoretical support for ecological restoration in the coal mine area.

1. Introduction

Land degradation is a seriously environmental and ecoligical problem facing the world due to human activities and climate change, which could decrease the land productivity and increase landscape fragmentation[1, 2]. Moreover, the ecological environment in Loess Plateau is extremely fragile thus land degradation could be easily caused by coal mining activities, such as excavation and occupation[3].

Land degradation mainly focuses on carbon source/carbon sink[4-6], vegetation restoration[7, 8], and ecological reconstruction[9, 10]. With the RS and GIS, studies on land degradation in mine areas have achieved great progress[11-14]. The Global Assessment of Human-induced Soil Degradation (GLASOD) is the first to define land degradation as the deterioration or complete loss of soil product and is divided into four types: water erosion, wind erosion, physics and chemistry[13]. Later, Artificial under Asian Assessment for Soil Degradation (ASSOD) is proposed, and the Multi-Factor Land Degradation Comprehensive Assessment Method proposed by the Russian Academy of Sciences (RUSSIA)[12]. The analysis of land degradation mostly focuses on soil quality[15-17], ecological health[8], landscape scale[10], etc. However, the process of land degradation is complex. And dynamic monitoring is still hard to be achieved as the most study of land degradation is limited to small-scale sampling, so[18, 19].

The loess plateau located in the arid and semi-arid environment, is prone to soil erosion, desertification due to mining activities[20]. However, there are few studies about land degradation in this region, especially from the perspective of external characteristics. The previous study analyzed land damage, soil erosion and vegetation change from the perspective of land degradation characteristics, which provided a good idea for the research[12]. Therefore, Landsat 8 OLI remote sensing images were to being interpreted to identify the main external characteristics of soil erosion, desertification, and vegetation degradation. Then the *Normalized Different Vegetation Index* (NDVI) was selected as the proxy index, and the weight of different external index was determined by *Principal Component Analysis* (PCA). And land degradation grading model in Loess Plateau coal mine area was constructed. The results in the Xunyao coal mine area (XCMA) could be provided a theoretical basis for land degradation in Loess Plateau.

2. Materials and Methods

2.1.Study Area

XCMA belongs to Xunyi County of Xianyang city, Chunhua County and Yaozhou district of Tongchuan City in Shaanxi province, with a total area of about 1127 km^2 located in Huanglong. The terrain of the mining area is high in the west and low in the east, with the highest elevation of 1627.7m, the lowest point of 1216.9m, and the elevation difference of about 410.8m.

Meanwhile, XCMA belongs to the warm temperate semi-arid continental climate, with 9.2℃ of the annual average temperature, 634mm of annual average rainfall, but greater than 1000 mm of the annual average evaporation. The geomorphic types of XCMA are complex and diverse. The parent soil of XCMA is quaternary loess, and there are also calenders, sandstone, shale, limestone, and other bedrock and weathered residual slope deposits. Therefore, its coal seam occurrence is relatively stable. The main coal seam is 4-2 coal seams, with the resource reserves are about 800 million tons. Figure 1 shows the location of the XCMA.

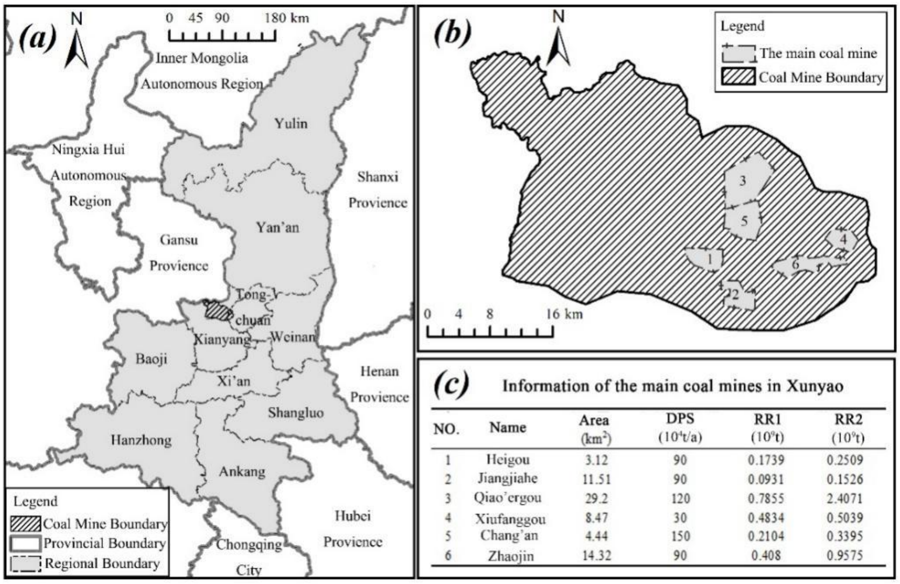

NO.	Name	Area (km^2)	DPS ($10^4 t/a$)	RR1 ($10^9 t$)	RR2 ($10^9 t$)
1	Heigou	3.12	90	0.1739	0.2509
2	Jiangjiahe	11.51	90	0.0931	0.1526
3	Qiao'ergou	29.2	120	0.7855	2.4071
4	Xiufanggou	8.47	30	0.4834	0.5039
5	Chang'an	4.44	150	0.2104	0.3395
6	Zhaojin	14.32	90	0.408	0.9575

Figure 1: Location of the study area. (a) Location of the XCMA in Shaanxi Province, China; (b) Distribution of the main coal mines in XCMA; (c) Information of the main coal mines in XCMA: DPS, designed production scale; RR1, recoverable reserves; RR2, resources reserves.

XCMA's main coal mines are underground mining. Unlike open-pit mining which could directly and severely disturb the ground surface[7, 21], the land degradation caused by mining impact directly is harder to assess in this region. But the effects of surface subsidence, meteorite pressure, and underground water decline due to mining has been calculated by predictive models[16, 22]. Therefore, we take XCMA as a study area to analyze t land degradation in the coal mining area from the perspective of external characterization.

2.2. Methods

2.2.1. Data Source and Pre-treatment

Table 1: Research data.

Data Type	Time	Identification	Resolution	Data Source
Landsat 8 OLI	2013-09-13	LC81270362013256LGN00	15 m	USGS
Landsat 8 OLI	2015-07-01	LC81270362015182LGN00	15 m	USGS
Landsat 8 OLI	2017-10-26	LC81270362017299LGN00	15 m	USGS
DEM	2009	ASTGTM_N34E108	30 m	GDC
DEM	2009	ASTGTM_N35E108	30 m	GDC
HWSD	2009	Harmonized World Soil Database(HWSD version1.1)	1 km	CDASDC
CGCD	2013-2017	SURF_CLI_CHN_MUL_MON	/	NMICC

Note: The full name of USGS is the United States Geological Survey (https://www.usgs.gov/); the full name of GDC is Geospatial Data Cloud (http://www.gscloud.cn/);the full name of CDASDC is Cold and Dry Area Science Data Center (http://www.gscloud.cn/); and the full name of NMICC is National Meteorological Information Center of China (http://data.cma.cn/).

The research data includes Landsat 8 OIL remote sensing image, Digital Elevation Model (DEM), the Harmonized World Soil Database (HWSD, version 1.1), and China Ground Climate Data Monthly Value Dataset (CGCD). Table 1 shows the research data. Among them, XCMA's

3-year(2013, 2015, 2017) Landsat 8 OIL images with no cloud, fog and good vegetation growth (July-October) were selected and pre-processed (including radiometric calibration, atmospheric correction, image fusion, image cropping). The attribute table of HWSD is associated with resampling to 30m, and the study area was extracted by the mask.

2.2.2. Methods

Land degradation is the result of the joint action of nature and human activities, and its variety of forms including but not limited to soil erosion, land desertification, soil secondary salinization, land pollution, vegetation degradation [23, 24]. Considering the reality of the loess plateau [20], soil erosion, desertification, and vegetation degradation are the mainly external characteristics. Thus, the precipitation, soil erodibility, slope and length, vegetation coverage, soil and water conservation measures, and land desertification impact factors are selected, and the results of vegetation coverage, soil erosion, and desertification could be calculated. NDVI value was taken as a reference, and principal component analysis (PCA) was chosen to calculate the weights of each characterization. Among them, vegetation coverage is a negative indicator, while desertification and soil erosion are a positive indicator of land degradation. According to the weight results, the grading model of land degradation in the loess coal mine area is constructed, while the graded results could be obtained.

(1) Calculation of vegetation coverage. The mixed pixel decomposition model was selected and the binary pixel model was used for linear decomposition. Based on the NDVI values of removed outliers and bare soil, vegetation coverage could be calculated [7, 25]. Combined with the classification methods of Ding et al., vegetation coverage is divided into five grades: Bare Land (BL), Low Coverage (LC), Medium Coverage (MC), Mid-high Coverage (MHC) and High coverage (HC). Since vegetation coverage is a negative indicator of land degradation, the resampling from bare land to high coverage is 5~1 in ArcGIS 10.6.

(2) Measurement of desertification degree. Using NDVI-Albedo to analyze desertification has the advantages of simple operation, easy acquisition and high result accuracy [26]. Therefore, desertification information of coal mine area could be extracted through this way based on Landsat 8 OLI image in ENVI 5.3 [27, 28]. The desertification degree is usually divided into 5 levels: No Desertification (ND), Mild Desertification (MID), Moderate Desertification (MOD), Severe Desertification (SD) and Extremely Severe Desertification (ESD). Then the desertification results assigned as 1~5 for resampling in ArcGIS 10.6.

(3) Calculation of soil erosion. The soil loss equitation (RUSLE) has been using to analyzed soil erosion [29]. In the equation, 6 factors of soil erosion were selected and calculated, then the erosion results could be obtained by using the grid calculator in ArcGIS 10.6. The RUSLE equation is shown in Equation 1:

$$A=R\times K\times LS\times C\times P \quad (1)$$

In Equation 1, A is the soil erosion modulus (Unit: t/hm2·a), R is the rainfall erosivity factor (Unit: MJ•mm/(hm2•h•a)), and K is the soil erodibility factor (Unit: t •h/ MJ•mm), S is the slope factor (dimensionless), L is the slope length factor (dimensionless), C is the vegetation cover management factor (dimensionless), and P is the soil and water conservation measure factor (dimensionless). The resampling is assigned a value of 1-6 in ArcGIS 10.6. According to the Soil Erosion Classification and Classification Standard (SL190-2007) promulgated by the Ministry of Water Resources of China, the degree of soil erosion is divided into 6 grades: Micro Erosion (MIE), Light Erosion(LE), Moderate Erosion(MOE), Strength Erosion(SE), Extreme strength Erosion(ESE), and Severe Erosion(SEE).

(4) Comprehensive evaluation and grading of land degradation. NDVI is often used as a proxy

for assessing land degradation in relation to the light energy efficiency of vegetation [30]. Based on the NDVI value, the PCA analysis of the reclassified vegetation degradation, desertification, and soil erosion weights were calculated in ArcGIS 10.6. Then the results of land degradation could be obtained. The calculation formula is shown in Equation 2.

$$LD = a_1 \bullet B_1 + a_2 \bullet B_2 + a_3 \bullet B_3 \quad (2)$$

In Equation 2, LD is land degradation results. And a_1, a_2 and a_3 are the weights of vegetation degradation, desertification, and soil erosion, respectively; B_1, B_2, and B_3, corresponding to the classification result values. All units are dimensionless. The value of LD ranges from 1 to 6. With reference to previous research results[14, 31], the degree of land degradation is divided into 4 levels: No Degradation (NDE, 1.0-1.8), Mild Degradation (MIDE, 1.8-3.1), Moderate Degradation (MODE, 3.1-4.4), Severe degradation (SDE, 4.4-6.0).

3. Results

3.1. Vegetation Coverage Calculation Results

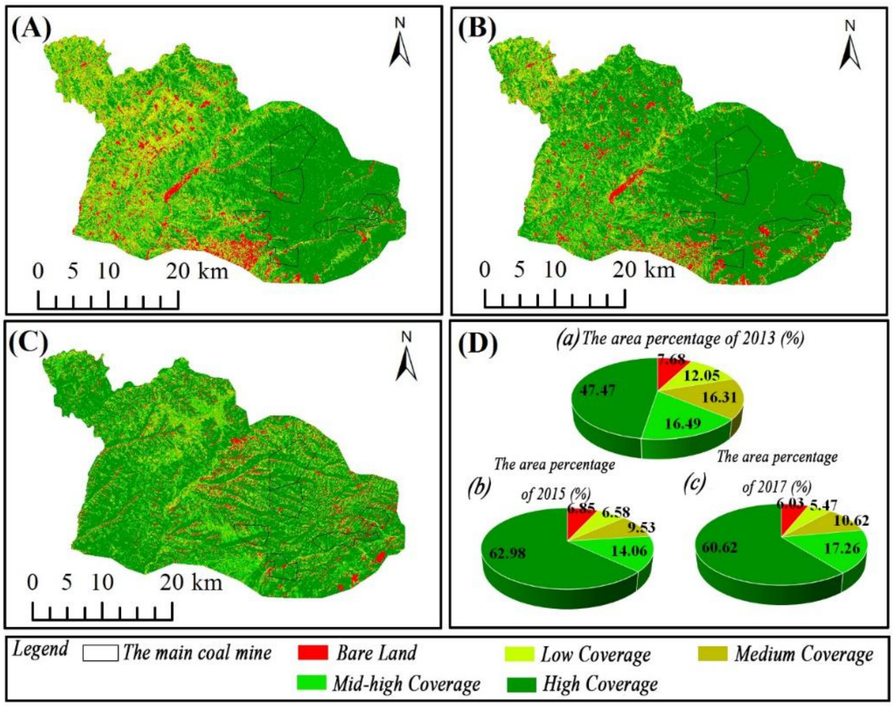

Figure 2: Results of vegetation coverage in XCMA. (A), (B), and (C) are the vegetation coverage maps of 2013, 2015, and 2017; and (a), (b), and (c) of (D) corresponds to the percentage of the vegetation coverage area.

Figure 2 shows the results of XCMA vegetation coverage. The BL and LC area decreased by 18.51 and 74.04 km2 respectively in 2013~2017. The MC and MHC increased first and then decreased. And MC decreased by 63.99 km2 while MHC increased by 8.77 km2; HC decreased first and then increased, with totally increased by 148.66 km2. The vegetation coverage is high in the southeast and low in the northwest in space.

3.2. Desertification Degree Calculation Results

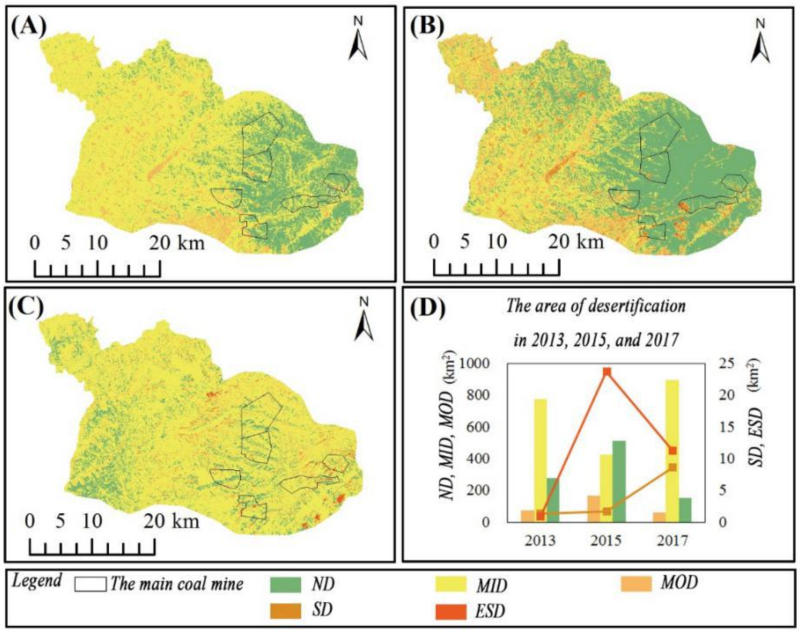

Figure 3: Results of desertification degree in XCMA. (A), (B), and (C) are the desertification distribution maps in 2013, 2015, and 2017, and (D) is the desertification area of the corresponding year.

Figure 3 shows the results of XCMA desertification degree calculation.In terms of quantity, the area of ND, MOD, and ESD increased first and then decreased, and the changes were -124.75, -11.46, and 7.35 km2 during 2013~2017, respectively. MID and SD increased first and then increased, and increased by 119.39 and 10.37 km2 respectively during 2013~2017. In terms of space, the distribution of desertification is light in the southeast but serious in the northwest.

3.3. Soil Erosion Calculation Results

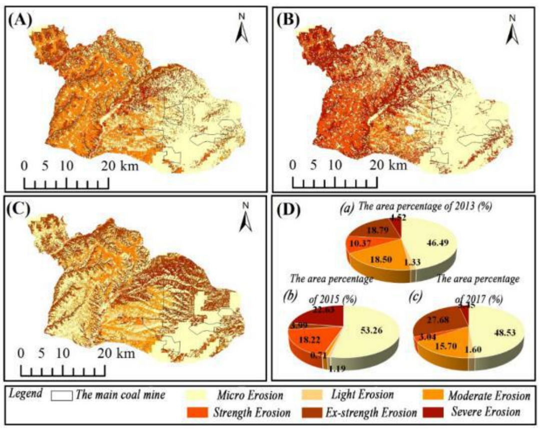

Figure 4: Results of soil erosion in XCMA. (A), (B), and (C) are the soil erosion distribution maps in 2013, 2015, and 2017, and (a), (b), and (c) of (D) corresponds to the percentage of soil erosion area.

Figure 4 shows the results of XCMA soil erosion calculation. In terms of quantity, ME, SE, and SEE increased first and then decreased with 22.97, -31.15, and -11.99 km2 changes from 2013 to

2017, respectively. LE, MOD, and ESE decreased first and then increased with 3.06, -81.90, and 99.44 km2 changes from 2013 to 2017, respectively. And soil erosion is generally weak in the southeast and strong in the northwest of spatial distribution.

3.4. Comprehensive Evaluation and Classification Results of Land Degradation

Table 2: External characterization of land degradation weight value results.

	Eigenvalue λ	Variance contribution rate (%)	Cumulative variance contribution rate (%)
Soil Erosion	7.625	69.66	69.66
Vegetation Coverage	3.753	18.28	87.94
Desertification	1.182	12.06	100.00

According to PCA analysis, the variance contribution rate and cumulative contribution rate for the vegetation coverage, desertification, soil erosion were calculated. Table 2 shows the eigenvalue, variance contribution rate and cumulative variance contribution rate of land degradation in 2013, 2015 and 2015.

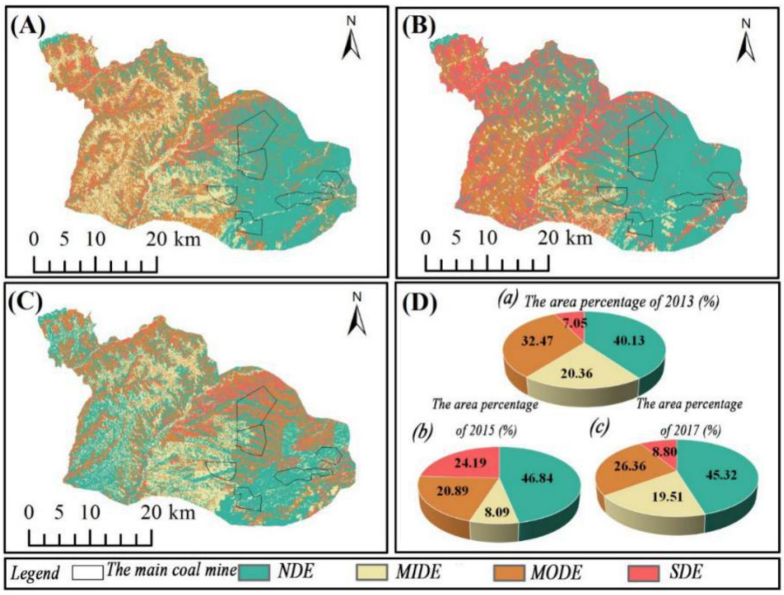

Figure 5: Land degradation classification results in XCMA. (A), (B), and (C) are the land degradation classification maps in 2013, 2015, and 2017, and (a), (b), and (c) for (D) correspond to the land degradation for 2013, 2015, and 2017. The proportion of degradation in grades is %.

4. Discussion

4.1. Analysis of External Characterization of Land Degradation

4.1.1. Vegetation Coverage

From the perspective of the coal mine area, the MCM is distributed on the southeast side in the XCMA, and the vegetation coverage is good in the mountain. From the perspective of coal mines, there is a large area of BL in the five major coal mines of Heigou, Jiangjiahe, Zhaojin, Xundong Chang'an and Xiufanggou, with the highest values accounting for 37.8%, 8.9% and 10.45% of the coal mines respectively. 7.3%, 6.1%. Combined with remote sensing image interpretation, the BL area is mainly mine area and drainage field. The vegetation coverage in the Qiaoergou coal mine is relatively good. In addition to the previous studies [32, 33], the vegetation degradation caused by the natural geographical environment is excluded, and the distance from the mining area, the drainage field, and the subsidence area are related to the vegetation coverage. That is, the closer to the mine working area, the lower the vegetation coverage, which could prove the results.

XCMA's main coal mines have the lowest vegetation coverage in 2015, followed by 2017 and relatively good in 2013, from the perspective of inter-annual change, Overall, vegetation coverage in the MCM range has declined, but it has improved in recent years. Combined with the study [34, 35], underground mining has a negative impact on vegetation cover and is related to the mining time, which can prove the results. In 2017, the vegetation coverage increased, and the result was caused by green filling and mining [36].

4.1.2. Desertification

The XCMA is generally in ND and MID. In terms of quantity, MOD, SD, and ESD appeared in the five coal mines of Heigou, Jiangjiahe, Zhaojin, Xundong Chang'an and Xiufanggou in 2013~2017. The proportion of the area of MOD, SD, and ESD reached 22.7%, 7.8%, 7.6%, 4.2%, and 3.2%, respectively. Among them, Zhaojin Coal Mine has a relatively low area of MOD, SD, and ESD, but both SD and ESD. In terms of spatial distribution, SD and ESD are mostly located in the mine working area, especially in the mining area. Combined with previous studies [37], coal resources disturbed the surface during mining and transportation, which intensified the development of desertification, consistent with the results of research and interpretation.

The degree of desertification in the mining area has increased in 2017. Although the overall degree of desertification was lower than that in 2017 in 2015, the area of SD and ESD was relatively large, and in 2013, the relative situation was relatively good. Similar to the results of previous studies, most of the coal mining areas are ESD, and coal mining is likely to cause ESD area expansion. The desertification growth area outside the coal mine area is mainly distributed around the coal mine, which is caused by unreasonable construction activities[38].

4.1.3. Soil Erosion

Soil erosion could be affected by climate, terrain slope, land use status, and soil properties [39]. In terms of quantity, the area of SE, ESE, and SSE in Qiaoergou Coal Mine, Xundong Chang'an Coal Mine and Hegou Coal Mine accounted for a relatively high proportion. The highest erosion intensity of Qiaoergou and Xundong Chang'an coal mine was 2017, the proportion of ESE and SSE area was 51.6% and 32.7%, respectively, while that of Hegou Coal Mine was 2015, accounting for 17.9%. Compared with the area of the unmined area of the mining area, the land use types such as cultivated land and forest land are most affected by soil erosion. Because the underground goaf forms an underground funnel, the groundwater in the unmined area is led to the goaf, which leads to the destruction of the hydrological pattern of the groundwater. This aggravates the changes in the physical and chemical properties of the surface soil in the unmined areas, resulting in greater soil erosion intensity in the unmined areas. Hu et al. have similar views of our results[40].

In terms of interannual variation and spatial distribution, soil erosion was relatively light in 2013, and the erosion range was mainly located in central construction land, forest land, rivers, etc.; soil erosion increased in 2015, and MOE, SE, ESE, and SSE areas were concentrated in cultivated land. The trend of soil erosion in 2017 is reduced within the scope of cultivated land, but it is further intensified in the scope of coal mines, and there is a tendency to gradually move to the forest land in the southeastern mountains. Compared with the results of soil erosion in 2013, 2015 and 2017, the differences in factors such as soil and water conservation, soil erodibility and slope length are small, and precipitation erosivity factors and vegetation cover factors are quite different. And Nigam et al. have a similar conclusion with this paper[39].

4.2. Analysis of Land Degradation

According to the results of PCA analysis, the soil erosion, vegetation cover, and desertification accounted for 0.6966, 0.1828 and 0.1206, respectively. In addition, land degradation refers to the process of degrading the land quality and productivity under adverse natural and human influences due to a combination of battalions or several types of battalions[1]. Therefore, NDVI could be selected as a proxy indicator for assessing land degradation[30]. Bian et al. proposed that the land use in the northwest coal mining area is mainly grassland and woodland, and soil erosion is dominated by hydraulic erosion[41]. In addition, the soil erosion in the Loess Plateau mainly occurs during the heavy rain period, while the research period is the season of abundant rainfall from July to October[20]. The soil erosion phenomenon is extremely serious under the influence of natural factors and human activities. Therefore, soil erosion has a greater weighting effect on land degradation. In 2013, the vegetation coverage was good and it was not in the dusty climate, so the impact factors were light.

Within the scope of major coal mines, land degradation was the most severe in 2017, especially in Qiaoergou Coal Mine and Chang'an Coal Mine. The area of MODE and SDE accounted for 43.8% and 37.6% of the total coal mine area respectively. In 2013, the degree of land degradation was low. Only 64% of the area of Heigou Coal Mine was in MODE, and most of the other coal mines were MIDE. In 2015, 17.8%, 6.6%, and 2.7% of the three coal mines in Qiaoergou, Xiufanggou, and Zhaojin began to exhibit SDE. The author has inferred two main reasons for land degradation on the Loess Plateau: First, high-intensity mining activities on the surface caused by land damage (excavation, occupation, collapse, etc.)[41], resulting in soil fertility decline, vegetation damage. In particular, the goaf is prone to changes in the groundwater pattern, which exacerbates the deterioration of the physical and chemical properties of the surface soil, and Mao's research can also prove the inference[1]. Second, the annual precipitation in the Loess Plateau is small, but the heavy rain during the flood season is concentrated and accounts for the annual precipitation. The proportion of the land is large, and the long-term soil erosion caused by debris, beams, ridges and valleys and other special geomorphological forms, resulting in ecological fragility and serious environmental damage, Zhen et al also made similar inferences[42]. Therefore, we should focus on artificially intervening vegetation restoration, scientifically carry out comprehensive management of small watersheds, and enhance the self-remediation function of ecosystems, so as to achieve sustainable development of soil and water conservation functions on the Loess Plateau.

5. Conclusion

NDVI was selected as the proxy indicator, and vegetation cover, desertification, and soil erosion were selected as three major external characterizations for PCA analysis, taking XCMA as an example. Starting from the perspective of external characterization of land degradation, the results of land degradation and grading are derived from the superposition analysis of weighted results.

The main conclusions are as follows: (1) Soil erosion, vegetation cover and desertification account for 0.6966, 0.1828 and 0.1206, respectively. And soil erosion caused by heavy rain during the flood season in the Loess Plateau is the main characterization for land degradation. (2) As for the overall area of the mining area, vegetation cover, desertification, soil erosion, and land degradation are all in the southeast and northwest. During 2013-2017, the changes of BL, LC, MC, MHC and HC were - 18.51, -74.04, -63.99, +8.77, +148.66 km^2, respectively. The changes of ND, MID, MOD, SD, ESD are -124.75, +119.39, -11.46, +10.37, +7.35 km^2, respectively. The changes of ME, LE, ME, SE, ESE, and SEE were +22.97, +3.06, -81.90, -31.15, -11.99, and +99.44 km^2, respectively. The changes of NDE, MIDE, MODE, and SDE are +58.70, -9.12, -67.73, and +19.68 km^2, respectively. (3) In a single coal mine, BL (vegetation cover impacts), SD and ESD (desertification impacts) are mainly located in the mining area and the drainage of the coal mine. The range of the unmined area will also have a certain impact due to the change of groundwater, and it would be affected by climate. Surface disturbance is the mean reason for land degradation of coal mining in the Loess Plateau.

Acknowledgments

This study was supported by the National Basic Work of Science and Technology of China (2014FY110800), National Key Research and Development Program of China (2016YFC0501107), and National Natural Science Foundation of China (U171010160).

References

[1] D. Mao, Z. Wang, B. Wu, Y. Zeng, L. Luo, B. Zhang. Land degradation and restoration in the arid and semiarid zones of China: Quantified evidence and implications from satellites. LAND DEGRAD DEV. 2018;29:3841-51.

[2] A. Grainger. Is Land Degradation Neutrality feasible in dry areas? J ARID ENVIRON. 2015;112:14-24.

[3] Q. Zhao, F. Guo, Y. Zhang, S. Ma, X. Jia, W. Meng. How sulfate-rich mine drainage affected aquatic ecosystem degradation in northeastern China, and potential ecological risk. SCI TOTAL ENVIRON. 2017;609:1093-102.

[4] J. Ahirwal, S.K. Maiti, A.K. Singh. Changes in ecosystem carbon pool and soil CO 2 flux following post-mine reclamation in dry tropical environment, India. SCI TOTAL ENVIRON. 2017;583:153-62.

[5] X. Chuai, X. Qi, X. Zhang, J. Li, Y. Yuan, X. Guo, et al. Land degradation monitoring using terrestrial ecosystem carbon sinks/sources and their response to climate change in China. LAND DEGRAD DEV. 2018;29:3489-502.

[6] Y. Hong, Y. Liu, Y. Chen, Y. Liu, L. Yu, Y. Liu, et al. Application of fractional-order derivative in the quantitative estimation of soil organic matter content through visible and near-infrared spectroscopy. GEODERMA. 2019;337:758-69.

[7] A. Erener. Remote sensing of vegetation health for reclaimed areas of Seyitömer open cast coal mine. INT J COAL GEOL. 2011;86:20-6.

[8] J.E. Herrick, P. Shaver, D.A. Pyke, M. Pellant, D. Toledo, N. Lepak. A strategy for defining the reference for land health and degradation assessments. ECOL INDIC. 2019;97:225-30.

[9] E. Rocha-Nicoleite, G.E. Overbeck, S.C. Müller. Degradation by coal mining should be priority in restoration planning. PERSPECT ECOL CONSER. 2017;15:202-5.

[10] J. Peng, Y. Pan, Y. Liu, H. Zhao, Y. Wang. Linking ecological degradation risk to identify ecological security patterns in a rapidly urbanizing landscape. HABITAT INT. 2018;71:110-24.

[11] M.A.E. AbdelRahman, A. Natarajan, R. Hegde. Assessment of land suitability and capability by integrating remote sensing and GIS for agriculture in Chamarajanagar district, Karnataka, India. The Egyptian Journal of Remote Sensing and Space Science. 2016;19:125-41.

[12] M.I. Gammal, R.R. Ali, R.M. Abou Samra. GIS-based land degradation risk assessment of Damietta governorate, Egypt. Egyptian Journal of Basic and Applied Sciences. 2015;2:183-9.

[13] S.K. Karan, S.R. Samadder, S.K. Maiti. Assessment of the capability of remote sensing and GIS techniques for monitoring reclamation success in coal mine degraded lands. J ENVIRON MANAGE. 2016;182:272-83.

[14] T. Vågen, L.A. Winowiecki, J.E. Tondoh, L.T. Desta, T. Gumbricht. Mapping of soil properties and land degradation risk in Africa using MODIS reflectance. GEODERMA. 2016;263:216-25.

[15] S. Mukhopadhyay, S.K. Maiti, R.E. Masto. Use of Reclaimed Mine Soil Index (RMSI) for screening of tree species for reclamation of coal mine degraded land. ECOL ENG. 2013;57:133-42.

[16] L. Huang, P. Zhang, Y. Hu, Y. Zhao. Vegetation succession and soil infiltration characteristics under different aged refuse dumps at the Heidaigou opencast coal mine. GLOB ECOL CONSERV. 2015;4:255-63.

[17] M. Zovko, D. Romić, C. Colombo, E. Di Iorio, M. Romić, G. Buttafuoco, et al. A geostatistical Vis-NIR spectroscopy index to assess the incipient soil salinization in the Neretva River valley, Croatia. GEODERMA. 2018;332:60-72.

[18] A.A.E. Baroudy, F.S. Moghanm. Combined use of remote sensing and GIS for degradation risk assessment in some soils of the Northern Nile Delta, Egypt. The Egyptian Journal of Remote Sensing and Space Science. 2014;17:77-85.

[19] M.A.E. AbdelRahman, A. Natarajan, C.A. Srinivasamurthy, R. Hegde. Estimating soil fertility status in physically degraded land using GIS and remote sensing techniques in Chamarajanagar district, Karnataka, India. The Egyptian Journal of Remote Sensing and Space Science. 2016;19:95-108.

[20] X. Liu, Z. Bai, W. Zhou, Y. Cao, G. Zhang. Changes in soil properties in the soil profile after mining and reclamation in an opencast coal mine on the Loess Plateau, China. ECOL ENG. 2017;98:228-39.

[21] L. Zhang, J. Wang, Z. Bai, C. Lv. Effects of vegetation on runoff and soil erosion on reclaimed land in an opencast coal-mine dump in a loess area. CATENA. 2015;128:44-53.

[22] W. Xiao, Y. Fu, T. Wang, X. Lv. Effects of land use transitions due to underground coal mining on ecosystem services in high groundwater table areas: A case study in the Yanzhou coalfield. LAND USE POLICY. 2018;71:213-21.

[23] V. Novianti, R.H. Marrs, D.N. Choesin, D.T. Iskandar, D. Suprayogo. Natural regeneration on land degraded by coal mining in a tropical climate: Lessons for ecological restoration from Indonesia. LAND DEGRAD DEV. 2018;29:4050-60.

[24] Z. Mekonnen, H. Taddese Berie, T. Woldeamanuel, Z. Asfaw, H. Kassa. Land use and land cover changes and the link to land degradation in Arsi Negele district, Central Rift Valley, Ethiopia. Remote Sensing Applications: Society and Environment. 2018;12:1-9.

[25] X. Liu, W. Zhou, Z. Bai. Vegetation coverage change and stability in large open-pit coal mine dumps in China during 1990–2015. ECOL ENG. 2016;95:447-51.

[26] R. Becerril-Piña, C.A. Mastachi-Loza, E. González-Sosa, C. Díaz-Delgado, K.M. Bâ. Assessing desertification risk in the semi-arid highlands of central Mexico. J ARID ENVIRON. 2015;120:4-13.

[27] D. Xu, C. Li, X. Song, H. Ren. The dynamics of desertification in the farming-pastoral region of North China over the past 10 years and their relationship to climate change and human activity. CATENA. 2014:11-22.

[28] J. Yang, Y. Wang. Estimating evapotranspiration fraction by modeling two-dimensional space of NDVI/albedo and day–night land surface temperature difference: A comparative study. ADV WATER RESOUR. 2011;34:512-8.

[29] M. Zerihun, M.S. Mohammedyasin, D. Sewnet, A.A. Adem, M. Lakew. Assessment of soil erosion using RUSLE, GIS and remote sensing in NW Ethiopia. Geoderma Regional. 2018;12:83-90.

[30] S. Piao, J. Fang, H. Liu, B. Zhu. NDVI-indicated decline in desertification in China in the past two decades. GEOPHYS RES LETT. 2005;32:347-54.

[31] G. Kust, O. Andreeva, A. Cowie. Land Degradation Neutrality: Concept development, practical applications and assessment. J ENVIRON MANAGE. 2017;195:16-24.

[32] S. Liu, W. Li, Q. Wang. Zoning method for environmental engineering geological patterns in underground coal mining areas. SCI TOTAL ENVIRON. 2018;634:1064-76.

[33] B. Vriens, H. Peterson, L. Laurenzi, L. Smith, C. Aranda, K.U. Mayer, et al. Long-term monitoring of waste-rock weathering at the Antamina mine, Peru. CHEMOSPHERE. 2019;215:858-69.

[34] A. Bechtel, A.I. Karayiğit, R.F. Sachsenhofer, H. İnaner, K. Christanis, R. Gratzer. Spatial and temporal variability in vegetation and coal facies as reflected by organic petrological and geochemical data in the Middle Miocene Çayirhan coal field (Turkey). INT J COAL GEOL. 2014;134-135:46-60.

[35] X.H.Z.L. LU. Vegetation Growth Monitoring Under Coal Exploitation Stress by Remote Sensing in the Bulianta Coal Mining Area. Journal of China University of Mining and Technology. 2007;17:479-83.

[36] S. LEI, Z. BIAN, J.L. DANIELS, X. HE. Spatio-temporal variation of vegetation in an arid and vulnerable coal mining region. Mining Science and Technology (China). 2010;20:485-90.

[37] D. Zhang, G. Fan, L. Ma, A. Wang, Y. Liu. Harmony of large-scale underground mining and surface ecological environment protection in desert district - a case study in Shendong mining area, northwest of China. Procedia Earth and Planetary Science. 2009;1:1114-20.

[38] L. Ma, D. Zhang, J. Jia, Y. Zhao, X. Cao, Z. Bo, et al. The recycling mode and technique of water in desertification area of Shendong Coal Mine. Energy Procedia. 2012;14:20-5.

[39] G.K. Nigam, R.K. Sahu, M.K. Sinha, X. Deng, R.B. Singh, P. Kumar. Field assessment of surface runoff, sediment yield and soil erosion in the opencast mines in Chirimiri area, Chhattisgarh, India. Physics and Chemistry of the Earth, Parts A/B/C. 2017;101:137-48.

[40] S. Hu, E. Wang, X. Li, B. Bai. Effects of gas adsorption on mechanical properties and erosion mechanism of coal. J NAT GAS SCI ENG. 2016;30:531-8.

[41] Z. Bian, W. Shen. Driving Factors of Land Degradation in Major Mining Areas in West China. Journal of Ecology and Rural Environment. 2016;32:173-7.

[42] Q. Zhen, W. Ma, M. Li, H. He, X. Zhang, Y. Wang. Effects of vegetation and physicochemical properties on solute transport in reclaimed soil at an opencast coal mine site on the Loess Plateau, China. CATENA. 2015;133:403-11.